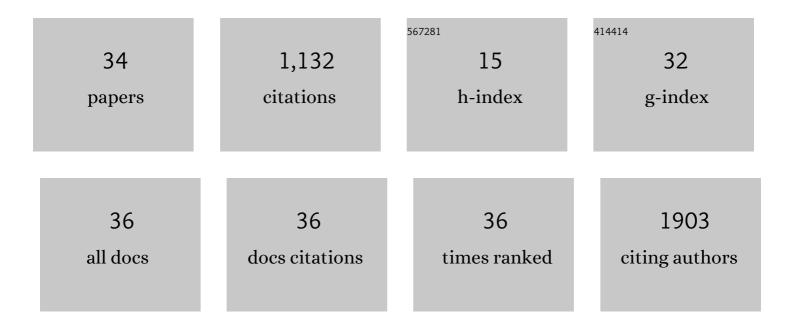
Scott W Lovell

List of Publications by Year in descending order

Source: https://exaly.com/author-pdf/3935231/publications.pdf Version: 2024-02-01



SCOTT W LOVEL

#	Article	IF	CITATIONS
1	<scp><i>PHIP</i></scp> gene variants with protein modeling, interactions, and clinical phenotypes. American Journal of Medical Genetics, Part A, 2022, 188, 579-589.	1.2	3
2	Structure-Guided Design of Potent Spirocyclic Inhibitors of Severe Acute Respiratory Syndrome Coronavirus-2 3C-like Protease. Journal of Medicinal Chemistry, 2022, 65, 7818-7832.	6.4	20
3	Structural insight into the novel ironâ€coordination and domain interactions of transferrinâ€1 from a model insect, <i>Manduca sexta</i> . Protein Science, 2021, 30, 408-422.	7.6	9
4	Structure–activity relationship of ipglycermide binding to phosphoglycerate mutases. Journal of Biological Chemistry, 2021, 296, 100628.	3.4	2
5	Structure-Guided Design of Conformationally Constrained Cyclohexane Inhibitors of Severe Acute Respiratory Syndrome Coronavirus-2 3CL Protease. Journal of Medicinal Chemistry, 2021, 64, 10047-10058.	6.4	38
6	Postinfection treatment with a protease inhibitor increases survival of mice with a fatal SARS-CoV-2 infection. Proceedings of the National Academy of Sciences of the United States of America, 2021, 118, .	7.1	61
7	Structure-Guided Design of Potent Inhibitors of SARS-CoV-2 3CL Protease: Structural, Biochemical, and Cell-Based Studies. Journal of Medicinal Chemistry, 2021, 64, 17846-17865.	6.4	22
8	Structural and ligand binding analyses of the periplasmic sensor domain of RsbU in Chlamydia trachomatis support a role in TCA cycle regulation. Molecular Microbiology, 2020, 113, 68-88.	2.5	11
9	Structure of the Diphtheria Toxin at Acidic pH: Implications for the Conformational Switching of the Translocation Domain. Toxins, 2020, 12, 704.	3.4	8
10	3C-like protease inhibitors block coronavirus replication in vitro and improve survival in MERS-CoV–infected mice. Science Translational Medicine, 2020, 12, .	12.4	187
11	The Structures of SctK and SctD from Pseudomonas aeruginosa Reveal the Interface of the Type III Secretion System Basal Body and Sorting Platform. Journal of Molecular Biology, 2020, 432, 166693.	4.2	14
12	Crystal Structure of VapBC-1 from Nontypeable Haemophilus influenzae and the Effect of PIN Domain Mutations on Survival during Infection. Journal of Bacteriology, 2019, 201, .	2.2	5
13	Using disruptive insertional mutagenesis to identify the <i>in situ</i> structureâ€function landscape of the <i>Shigella</i> translocator protein IpaB. Protein Science, 2018, 27, 1392-1406.	7.6	13
14	Structure-guided design of potent and permeable inhibitors of MERS coronavirus 3CL protease that utilize a piperidine moiety as a novel design element. European Journal of Medicinal Chemistry, 2018, 150, 334-346.	5.5	96
15	Bfd, a New Class of [2Fe-2S] Protein That Functions in Bacterial Iron Homeostasis, Requires a Structural Anion Binding Site. Biochemistry, 2018, 57, 5533-5543.	2.5	8
16	Macrocycle peptides delineate locked-open inhibition mechanism for microorganism phosphoglycerate mutases. Nature Communications, 2017, 8, 14932.	12.8	41
17	Structural characterization of the Man5 glycoform of human IgG3 Fc. Molecular Immunology, 2017, 92, 28-37.	2.2	21
18	Single-domain antibodies pinpoint potential targets within Shigella invasion plasmid antigen D of the needle tip complex for inhibition of type III secretion. Journal of Biological Chemistry, 2017, 292, 16677-16687.	3.4	16

SCOTT W LOVELL

#	Article	IF	CITATIONS
19	Structure-based exploration and exploitation of the S4 subsite of norovirus 3CL protease in the design of potent and permeable inhibitors. European Journal of Medicinal Chemistry, 2017, 126, 502-516.	5.5	20
20	1.45â€Ã resolution structure of SRPN18 from the malaria vector <i>Anopheles gambiae</i> . Acta Crystallographica Section F, Structural Biology Communications, 2016, 72, 853-862.	0.8	3
21	Crystal structure of histone-like protein fromStreptococcus mutansrefined to 1.9â€Ã resolution. Acta Crystallographica Section F, Structural Biology Communications, 2016, 72, 257-262.	0.8	4
22	Replacing Arginine 33 for Alanine in the Hemophore HasA from <i>Pseudomonas aeruginosa</i> Causes Closure of the H32 Loop in the Apo-Protein. Biochemistry, 2016, 55, 2622-2631.	2.5	12
23	1.65â€Ã resolution structure of the AraC-family transcriptional activator ToxT from <i>Vibrio cholerae</i> . Acta Crystallographica Section F, Structural Biology Communications, 2016, 72, 726-731.	0.8	13
24	Hypothetical protein <scp>CT</scp> 398 (<scp>C</scp> ds <scp>Z</scp>) interacts with σ ⁵⁴ (<scp>R</scp> po <scp>N</scp>)â€holoenzyme and the type III secretion export apparatus in <i>Chlamydia trachomatis</i> . Protein Science, 2015, 24, 1617-1632.	7.6	23
25	Structure-Guided Design and Optimization of Dipeptidyl Inhibitors of Norovirus 3CL Protease. Structure–Activity Relationships and Biochemical, X-ray Crystallographic, Cell-Based, and In Vivo Studies. Journal of Medicinal Chemistry, 2015, 58, 3144-3155.	6.4	51
26	Structural and Inhibitory Effects of Hinge Loop Mutagenesis in Serpin-2 from the Malaria Vector Anopheles gambiae. Journal of Biological Chemistry, 2015, 290, 2946-2956.	3.4	7
27	Characterization of the Bacterioferritin/Bacterioferritin Associated Ferredoxin Protein–Protein Interaction in Solution and Determination of Binding Energy Hot Spots. Biochemistry, 2015, 54, 6162-6175.	2.5	28
28	Structural and Biochemical Characterization of Chlamydia trachomatis Hypothetical Protein CT263 Supports That Menaquinone Synthesis Occurs through the Futalosine Pathway. Journal of Biological Chemistry, 2014, 289, 32214-32229.	3.4	23
29	1.15â€Ã resolution structure of the proteasome-assembly chaperone Nas2 PDZ domain. Acta Crystallographica Section F, Structural Biology Communications, 2014, 70, 418-423.	0.8	7
30	High-resolution crystal structures of two crystal forms of human cyclophilin D in complex with PEG 400 molecules. Acta Crystallographica Section F, Structural Biology Communications, 2014, 70, 717-722.	0.8	5
31	A potential regulatory loop between Lin28B:miR-212 in androgen-independent prostate cancer. International Journal of Oncology, 2014, 45, 2421-2429.	3.3	34
32	Structure/Function Relationships of Adipose Phospholipase A2 Containing a Cys-His-His Catalytic Triad. Journal of Biological Chemistry, 2012, 287, 35260-35274.	3.4	45
33	Broad-Spectrum Antivirals against 3C or 3C-Like Proteases of Picornaviruses, Noroviruses, and Coronaviruses. Journal of Virology, 2012, 86, 11754-11762.	3.4	277
34	Potent Protease Inhibitors of Highly Pathogenic Lagoviruses: Rabbit Hemorrhagic Disease Virus and European Brown Hare Syndrome Virus. Microbiology Spectrum, 0, , .	3.0	1